

Spatiotemporal chaos in a differential flow reactor

John H. Merkin,^a Razvan A. Satnoianu^{a,b} and Stephen K. Scott^{b*}

^a Department of Applied Mathematics and ^b School of Chemistry, University of Leeds, Leeds, UK LS2 9JT

The spatiotemporal evolution of a chemical system close to a Hopf bifurcation in a differential flow reactor is studied. The interaction of the Hopf-differential flow induced instabilities for the cubic autocatalator model is determined through the appropriate form of the complex Ginzburg–Landau equation for the evolving amplitude. New behaviour, including spatiotemporal chaos, is observed from this equation. These predictions are shown also to be a feature of the initial-value problem for the original autocatalator equations.

Diffusion is generally associated with the decay of imposed concentration gradients, leading to spatially uniform concentrations at long times. In 1952, Turing predicted¹ that, if selective diffusion occurs in a reacting system with feedback kinetics, then such a system may develop in the opposite sense, with an initially spatially uniform state becoming unstable to small perturbations and a spatial dependence of species concentrations developing spontaneously. Similar predictions had been made earlier by Rashevski.² Such Turing–Rashevski patterns require that the diffusivity of the feedback species should be sufficiently lower than that of the other species involved in the reaction. This prediction was originally made in the context of the development of spatial form, or morphogenesis, in biological systems but caused much interest amongst chemists,³ as oscillatory reactions became accepted, and also amongst mathematical biologists, where the ideas were extended as a basis for animal coat patterns.⁴ For recent reviews see ref. 5–7.

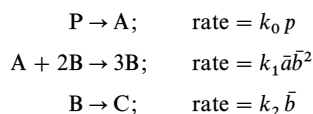
One potential hurdle to the experimental realisation of such patterns was the condition on the diffusion coefficients. No obvious method for selectively altering the diffusion coefficient of a single species in a mixture of reactants was known. This hurdle has recently been overcome in a relatively systematic way by using gelled media in which bulky complexing agent molecules are effectively immobilised and which selectively bind the required feedback species reducing its overall mobility.^{8–10} During the search for such techniques, alternative methods for creating spatial patterns through differential mobility were proposed. Pre-eminent among these is the differential flow system proposed by Rovinsky and Menzinger.^{11,12} They showed that a differential flow induced chemical instability (DIFICI) arises if a system with feedback kinetics is flowed through an open reactor, such that one of the reacting species has a lower characteristic flow velocity than the others. In general, there will be some critical flow rate beyond which spatial structure will develop spontaneously in the system. Spatial patterns in the form of propagating ‘bands’ of oxidation were obtained experimentally using the Belousov–Zhabotinsky (BZ) reaction in such a differential flow reactor. The reactants were flowed along a tube packed with a cation exchange resin on which the redox catalyst ferroin is immobilised. The oxidised form of the redox catalyst is the ‘resetting’ species for the chemical clock in this reaction and is thus arranged to have effectively zero flow compared to the autocatalyst HBrO_2 and inhibitor Br^- .

The DIFICI system thus offers an experimentally viable method of developing spatial concentration profiles in chemical systems. The propagating bands of the BZ system represent perhaps the simplest spatial structure in this reactor,

other than just the spatially uniform steady state. Here, we investigate the nature of other spatial patterns that may develop with the DIFICI system for a model chemical reaction which itself is capable of supporting simple oscillatory behaviour. The governing equations for this model in a differential flow reactor are given in the next section. Concentrating on the parameter values at which both the oscillatory (Hopf) and DIFICI bifurcations occur close together, we derive the corresponding complex Ginzburg–Landau (CGL) equation governing the evolution of the amplitude of the spatial concentration distribution. The effect of the DIFICI–Hopf interaction is to produce travelling wave packets in which the system locally moves away from the uniform steady state and then eventually returns to it. Analytical expressions for the speed at which the wave packet propagates and for the rate at which it grows in extent are derived in terms of the kinetic and flow parameters. Numerical computations confirm these predictions and also indicate the growth of a region of complex spatiotemporal behaviour, showing a sensitive dependence on initial conditions, at the centre of the wave packet. Finally, we return to the equations for the specific chemical model and show that this spatiotemporal chaos is also a feature of the initial-value problem for this scheme.

Model and governing equations

The cubic autocatalator model¹³ comprises the following reaction steps:



where p , \bar{a} and \bar{b} are the concentration of the reacting species and the k_i represent the reaction rate coefficients. We imagine a differential flow reactor fed with an inflow of pure P and in which species A is effectively immobile. The autocatalyst B is able to diffuse and flow through the reactor at a constant velocity u . With the further assumption that the reactor is sufficiently long for end effects to be ignored and sufficiently narrow so that there are no transverse variations in concentration, the resulting mass balance equations can be written in the following form

$$\frac{\partial \bar{a}}{\partial t} = k_0 p_0 - k_1 \bar{a} \bar{b}^2 \quad (1)$$

$$\frac{\partial \bar{b}}{\partial t} = D_B \frac{\partial^2 \bar{b}}{\partial x^2} - u \frac{\partial \bar{b}}{\partial x} + k_1 \bar{a} \bar{b}^2 - k_2 \bar{b} \quad (2)$$

where \bar{t} and \bar{x} are time and distance, respectively. Here we have made the usual ‘pool chemical approximation’ of the precursor reactant, regarding its concentration p_0 as constant in both space and time and equal to the inflow value. The justification of doing so for this particular model, in general terms, has been rigorously established elsewhere.¹⁴ These equations can be written in dimensionless variables as

$$\frac{\partial a}{\partial t} = \mu - ab^2 \quad (3)$$

$$\frac{\partial b}{\partial t} = \frac{\partial^2 b}{\partial x^2} - \phi \frac{\partial b}{\partial x} + ab^2 - b \quad (4)$$

on $-\infty < x < \infty$ for $t > 0$. The following initial and boundary conditions are appropriate for the model

$$a(x, 0) = \mu^{-1}, b(x, 0) = \mu; \text{ on } -\infty \leq x \leq \infty \quad (5)$$

and

$$\partial b / \partial x \rightarrow 0 \text{ as } x \rightarrow \infty, t > 0 \quad (6)$$

Here, $a = \bar{a}/c_{\text{ref}}$, $b = \bar{b}/C_{\text{ref}}$ where $c_{\text{ref}} = (k_2/k_1)^{1/2}$, $t = k_2\bar{t}$, $\mu = k_0 p_0/k_2 c_{\text{ref}}$, $\phi = u/(k_2 D_B)^{1/2}$ and $x = \bar{x}/x_{\text{ref}}$ with $x_{\text{ref}} = (D_B/k_2)^{1/2}$. In what follows, the dimensionless flow rate ϕ and the reactant concentration μ are treated as the primary bifurcation parameters.

We also note that eqn. (3)–(6) have the spatially uniform steady state solution $S = \{a, b\} = \{\mu^{-1}, \mu\}$ and that, for the corresponding well stirred system, this solution is temporally stable for $\mu > 1$, with a supercritical Hopf bifurcation occurring at $\mu = 1$ and a stable limit cycle emerging around the unstable steady state for $\mu < 1$.

We are interested in the evolution of the system described by eqn. (3)–(6), subject to a small localised perturbation in the concentrations at $t = 0$. It has already been established that, for flow rates in excess of some critical value, $\phi > \phi_c$, there is a range of wavenumbers k in the Fourier transform of the linearised versions of eqn. (3) and (4), such that the steady state S is unstable to small localised perturbations composed of these wavenumbers.¹⁵ This critical flow rate ϕ_c is given by the minimum on the neutral curve

$$\phi^2 = \frac{(k^2 + \mu^2 - 1)^2(1 + k^2)}{k^2(1 - k^2)}, 0 < k < 1, \mu > 1 \quad (7)$$

In the vicinity of the Hopf point, we can derive an approximate expression for ϕ_c as μ tends to 1 from above:

$$\phi_c \sim 2\sqrt{2}|\mu - 1|^{1/2} + \dots, \mu \rightarrow 1 \quad (8)$$

For initial reactant concentrations close to the spatially homogeneous Hopf bifurcation, therefore, we expect small flow rates to modulate the oscillating Hopf pattern of the full system (3)–(6). To examine this, we can conveniently make use of the corresponding CGL equation for this system.

Reduction to CGL form

Elsewhere,¹⁶ we present the rigorous derivation of the CGL for the Hopf-DIFICI interaction valid for μ close to 1 in this model. Briefly, we take $\mu = 1 + r\epsilon^2$ with ϵ small and $r = \pm 1$ and introduce the scaled flow rate ψ , distance s and time τ defined by $\phi = \epsilon\psi$, $s = \epsilon x$ and $\tau = \epsilon^2 t$, respectively. The evolution of the concentration variables a and b is assumed to be given by an expansion of the form

$$a = a_0 + \epsilon a_1(s, \tau, t) + \dots \quad (9a)$$

$$b = b_0 + \epsilon b_1(s, \tau, t) + \dots \quad (9b)$$

with $(a_0, b_0) = (\mu^{-1}, \mu)$. The leading order terms a_1 and b_1 depend on the ‘long’ space and time variables s and τ and on the regular time t and can be expressed in terms of the

(complex) amplitude A , as

$$(a_1, b_1) = A(s, \tau)e^{it}(d_1, d_2) \quad (10)$$

where $d_1/d_2 = -2/(1 + i)$. The requirement that expansion (9) should remain uniform at $O(\epsilon^3)$ then leads, by the use of the method of multiple scales, for example, to the amplitude or CGL equation which has the form

$$\begin{aligned} \frac{\partial A}{\partial \tau} = & \frac{1 - i}{2} \frac{\partial^2 A}{\partial s^2} - \psi \frac{1 - i}{2} \frac{\partial A}{\partial s} \\ & + r(-1 + i)A - (1 + \frac{3}{2}i)|A|^2 A \end{aligned} \quad (11)$$

on $-\infty < s < \infty$, $\tau > 0$ with $A = 0$ initially and subject to some localised input. Here $r = +1$ or -1 depending on whether μ is slightly greater or slightly less than the Hopf bifurcation value at $\mu = 1$. We consider only the case with $r = -1$.

The advantage of using ‘normal form’ equations such as eqn. (11) is that they allow a generic survey of the behaviour of a class of systems in which different instabilities interact. Eqn. (11) differs from the classic CGL form through the ‘convective’ term, involving ψ . This was anticipated¹⁷ by Rovinsky *et al.* through a heuristic analysis, but emerges here rigorously, with the added advantage that there is immediate explicit correspondence with the physical, initial-value problem for the cubic autocatalator model.

Travelling wave solutions

One class of solutions¹⁸ of the CGL is that of travelling waves (TWS) which have the form $A(s, \tau) = A_s \exp(\omega\tau - iks)$ where A_s is a small constant. Substituting this into the linearised version of eqn. (11) we obtain the dispersion relation

$$\omega(k) = -\frac{1 - i}{2}k^2 + \frac{1 + i}{2}\psi k + 1 - i \quad (12)$$

Instability of the uniform steady state S arises when $\text{Re}(\omega) > 0$. We have an open system of infinite extent which can show either absolute or convective instability. The uniform state, $A = 0$, here is absolutely unstable, *i.e.* small disturbances at some point s_0 grow in time at that point, for $\psi < 2\sqrt{2}$. For $\psi > 2\sqrt{2}$, the uniform state is convectively unstable¹⁹ so that the initial perturbation grows in amplitude, but also propagates away from the initial point S_0 , with the system at s_0 returning to the $A = 0$ state. The most unstable wavenumber in this situation is given by $k = \psi/2$ and has a group velocity v_g given by

$$v_g = \frac{d \text{Im}(\omega)}{dk} = \psi \quad (13)$$

The subsequent analysis can conveniently be performed in terms of a travelling wave co-ordinate $\xi = s - v\tau$ for which the frequency $\alpha(k)$ is given by

$$\alpha(k) = \omega(k) - ikv \quad (14)$$

where v is the velocity in this frame. The edges of the wave packet move with velocities v_1 and v_2 , given by

$$v_{1,2} = \psi \pm \sqrt{4 + \frac{1}{2}\psi^2} \quad (15)$$

with $v_2 > v_g > v_1$, so the system exhibits a growing region of perturbation from the uniform state propagating with an overall velocity $v_g = \psi$, with the front and rear propagating with speeds $v_2 > \psi$ and $v_1 < \psi$, respectively, so that the spatial extent of the disturbed region grows in time. We also note that $v_1 < 0$ for $\psi < 2\sqrt{2}$.

Numerical integration of eqn. (11) for specific values of ψ confirms these basic predictions. The evolution in space s of the amplitude $|A|$ is shown for a system with $\psi = 3.98$ in Fig.

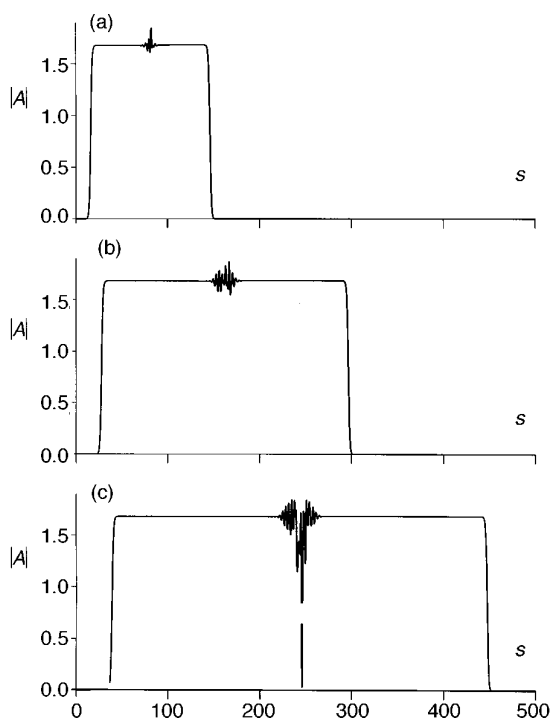


Fig. 1 Evolution of the amplitude $|A|$ of the CGL eqn. (11) with $\psi = 3.98$, showing the development of a travelling wave packet of non-zero amplitude with the front and rear edges propagating at different velocities relative to each other and to the group velocity (centre of the wave packet). A region of spatiotemporal complexity with THS is growing at the centre of the wave packet. Profiles are shown at equal time intervals (a) $\tau = 21.0$, (b) $\tau = 42.0$, (c) $\tau = 63.0$.

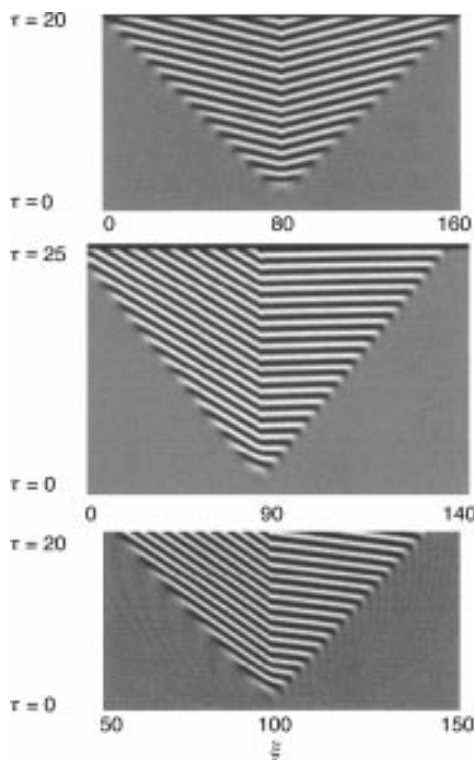


Fig. 2 Grey-scale contour plots showing the evolution of the amplitude $\text{Re}(A)$ in space and time for the CGL eqn. (11) with different flow parameters ψ . In each picture, dark areas corresponds to $\text{Re}(A) = 0$ and white corresponds to the maximum amplitude $\text{Re}(A)_{\text{max}}$: (a) $\psi = 0$, $\text{Re}(A)_{\text{max}} = 1.1$; (b) $\psi = 0.573$, $\text{Re}(A)_{\text{max}} = 1.2$; (c) $\psi = 1.0$, $\text{Re}(A)_{\text{max}} = 1.4$.

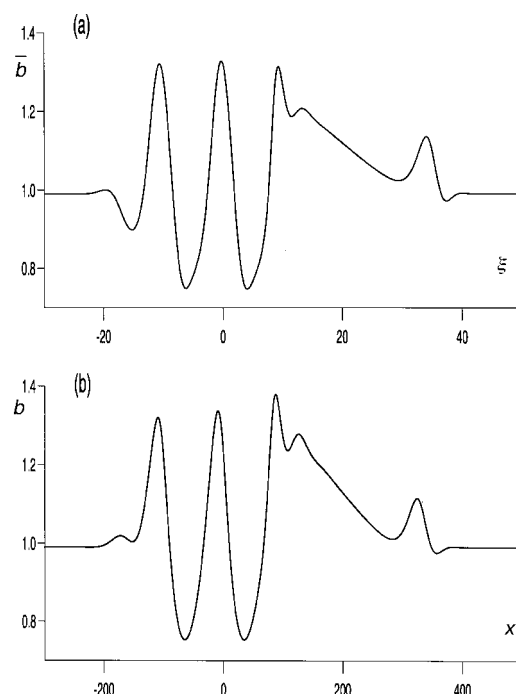


Fig. 3 Comparison of autocatalyst concentration profile (a) reconstructed from solution of CGL equation with $\psi = 0.573$, $\tau = 9.0$ and (b) from IVP for full kinetic model with $\mu = 0.99$ and $\phi = 0.0573$, $t = 900.0$ showing evolution of 'infinite wavelength' region behind the leading edge of the wave packet

1(a)–(c) for equal time intervals, after sufficient time has elapsed for the solution to develop fully. The initial state is the spatially uniform steady state S corresponding to $A = 0$. This is perturbed over a small region around $s = 0$ and a region or wave packet in which $|A|$ is non-zero is seen developing. The leading edge of the wave packet corresponds to the departure of the system from S and the trailing edge sees the return to S , with $|A| \rightarrow 0$, after the wave packet has passed through. Both edges propagate at different speeds from each other and from the packet itself, with the size of the wave packet increasing in time. The three velocities computed are in very good agreement with the analytical forms derived above. The rear of the wave packet is propagating with a low velocity, indicating the marginal convective instability for these parameter values. The wave packet has two regular sections in which the amplitude is constant, the amplitude of these two regions is also equal although they have different underlying wavelengths, separated by a region of irregular behaviour, increasing in extent and propagating with the group velocity. In Fig. 1(c) the amplitude has fallen back to near zero over a narrow range close to the centre of the wave packet. This feature is known as a travelling hole solution (THS).

With this information, we can now introduce the travelling wave coordinate $\xi = s - \psi\tau$ and look for solutions of eqn. (11), the so-called Stokes waves, of the form

$$A = R_i \exp[i(k_i \xi - \omega_i \tau)] \quad (16)$$

where R_i is a real constant and $i = 1$ for the rear part of the wave packet and $i = 2$ for the front part. The appropriate equations for R_i , ω_i and the wavenumbers k_i in terms of ψ can be obtained from the CGL by requiring that the solutions match the behaviour near the leading and rear edges of the wave packet and requiring neutral stability at these edges. We find that the phase velocity of the rear portion, relative to the group velocity, is negative with $k_1 < 0$ for all ψ , and $|k_1|$ increasing as the flow rate ψ increases. For the leading region, however, k_2 changes sign at $\psi = \psi_0$ where $\psi_0^2 = \frac{8}{3}(\sqrt{17} - 4)$,

i.e. $\psi_0 \approx 0.57296$, with $k_2 > 0$ for $\psi < \psi_0$. At ψ_0 , the direction of propagation of the waves in the front part of the packet changes direction relative to that of the wave packet itself. The analysis also confirms that the waves in the rear and front portions have the same amplitude. *i.e.* $R_1 = R_2$ for all ψ .

Contour plots of $\text{Re}(A)$ in the ξ - τ coordinate frame are shown in Fig. 2 for three values of the flow rate ψ , with $\psi = 0 < \psi_0$ in (a), $\psi = 0.573 \approx \psi_0$ in (b) and $\psi = 1.0 > \psi_0$ in (c). The different slopes of the wave profiles about the $\xi = 0$ axis indicate the different propagation speeds relative to the wave packet, with the change in direction also evident in the leading portion as ψ increases. In case (b) the infinite wavelength for the critical case ψ_0 can be seen in the leading portion. We can use the solution from the CGL equation to reconstitute the profile for the autocatalyst b from eqn. (9b). This is compared with the full solution of the initial-value problem for the corresponding parameters $\mu = 0.99$, $\phi = 0.0573$ in Fig. 3(a) and (b), respectively.

Spatiotemporal chaos

The remaining, major feature of the solutions to the CGL equation is the region of complex behavior connecting the regular front and rear portions of the TWS. The long-term evolution of the amplitude $|A|$ for the system with $\psi = 3.98$ computed from the CGL equation in the travelling wave coordinate ξ is shown in Fig. 4. Initially, $|A| = 0$, corresponding to the dark regions. A perturbation is imposed locally at $\xi = 0$ and the travelling wave solution develops through which $|A|$ tends to its maximum value $|A| = 1.824$, depicted in white. This leading wave develops symmetrically in this coordinate frame with constant velocity. As τ increases, however, in the vicinity of $\xi = 0$, the amplitude falls again in the centre of the wave packet, corresponding to the development of the complex transition region. In this region, the system develops THS, giving rise to profiles of the type shown previously in Fig. 1(c). The THS are travelling regions in which $|A| \approx 0$ acting as boundaries between different domains of higher amplitude. It has been suggested that these are 1D analogues of spiral cores for 2D systems.²⁰ The region of complex behaviour also grows essentially symmetrically at

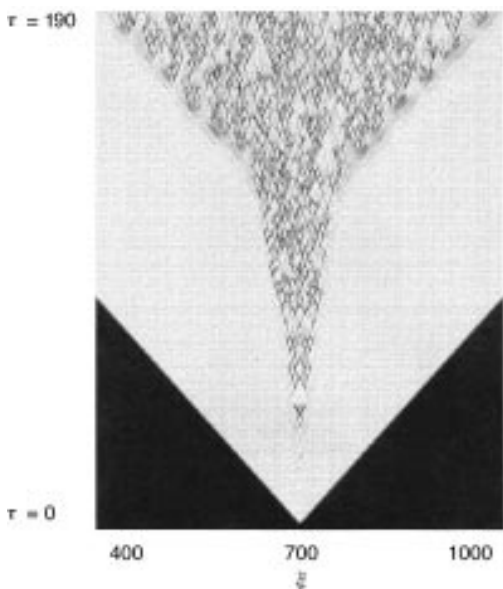


Fig. 4 Grey-scale contour plot showing the evolution of the amplitude $|A|$ in space and time for CGL equation with $\psi = 3.98$ showing initial wave packet development and subsequent growth of spatiotemporal complexity. Black corresponds to $|A| = 0$, white corresponds to $|A| = 1.824$.

early times, but with a velocity significantly lower than the leading TWS. THS solutions have been observed in CGL systems without the convective term and have been called 'amplitude turbulence'.^{21,22}

Eventually, there is a symmetry breaking bifurcation within the region of complex behaviour; this occurs approximately half-way up Fig. 4. Finally, we note that there is a third temporal scale on which there is a dramatic acceleration of the propagation of the irregular central region: the velocity of the leading edge of the THS region increases abruptly and becomes approximately equal to that of the TWS. At the same time, the system develops an interface region of small, apparently quasi-periodic waves which effect the transition from the regular TWS to the irregular THS.

Various diagnostic tests can be applied to these data in search of evidence for deterministic chaos. Perhaps the most important characteristic of a chaotic state is its sensitivity to initial conditions. Fig. 5 shows the development of the difference between two systems identical in parameter values and differing by only 1 part in 10^5 in the initial conditions at $s = 0$. The difference remains small outside the complex region at the centre of the wave packet, but grows rapidly therein, indicating the chaotic character.

The analytical connection between the CGL equation and the autocatalator model now allows us to seek the same complex spatio-temporal evolution in the initial-value problem (IVP) associated with the specific chemical kinetics. Spatial profiles for both systems at equivalent times are compared in Fig. 6(a) and (b). For the CGL equation we take $\psi = 3.98$ and show the reconstructed profile for the autocatalyst concentration at $\tau = 15$ over the range $s = 0$ to 90. If we assume, $\mu = 0.99$ for the autocatalator model, so $\varepsilon = 0.1$ with $r = -1$ the corresponding parameter values are $\phi = \varepsilon\psi = 0.398$, with $t = \tau/\varepsilon^2 = 1500$ over the region $0 < x < s/\varepsilon = 900$. (The computations for the IVP are relatively expensive so the integration has not been continued to very long times.)

A full quantitative match cannot be expected, not least because ε is not particularly small and ψ is not particularly close to zero, as assumed in the initial derivation of the CGL equation, but it is clear that there is good qualitative correspondence. Specifically, both systems show two regions of near constant amplitude at each end of the wave packet; the amplitudes of these two regions are effectively equal, but the wavelengths are different. Comparing the CGL and IVP solu-

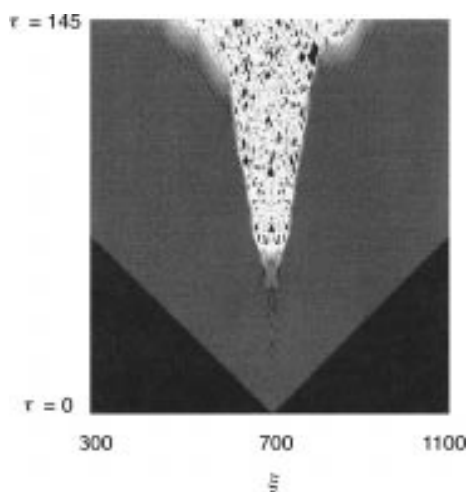


Fig. 5 Evolution of the absolute difference between the solution of the CGL equation for two systems with the same parameter values and boundary conditions differing only by one part in 10^5 in the initial perturbation at $\xi = 0$. The difference is shown on a logarithmic scale with $|A| \leq 10^{-7}$ in the darkest areas and $\leq 10^2$ in the white areas.

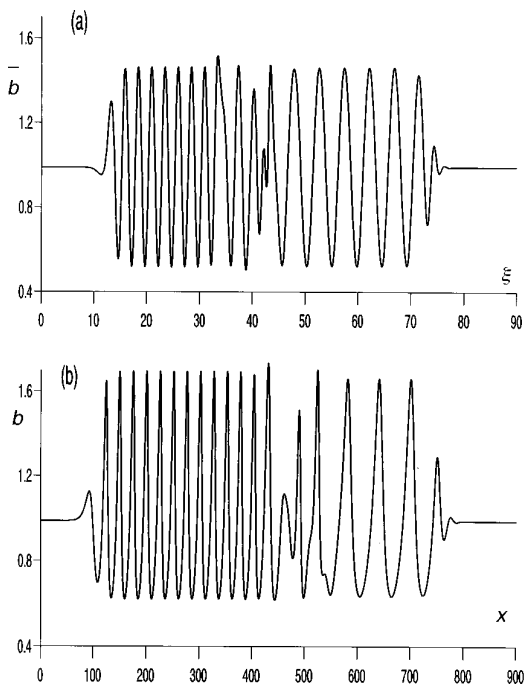


Fig. 6 Comparison of (a) reconstructed autocatalyst concentration for CGL eqn. (11) at $\tau = 15.0$ and (b) solution of IVP for cubic autocatalator model at $t = 1500$

tions in these regions, the wavelengths in the rear section of the wave packet are shorter than those in the front section in each case, though the wavelengths for the two systems differ only by order $O(\epsilon)$. In between, in each case, is a region of complex evolution. No simple match is expected here, not least because of the sensitivity of this chaotic evolution to initial conditions which are different in the CGL and IVP approaches. It is, nevertheless, clear that similar spatial complexity is a feature of the IVP equations.

Discussion

The results above describe the evolution of a differential flow system under experimental conditions close to the onset of spontaneous oscillation (Hopf bifurcation) in the reaction kinetics. Initially, the system is taken to be at the (temporally unstable) steady state and a small perturbation is made locally at the origin. This perturbation grows so that the system departs locally from the steady state but, because of the flow, is also convected along the reactor. At any given point (in the laboratory frame) therefore, the sequence is: an initial period during which the system remains at the steady state; the arrival of the leading front which causes the system to evolve away from the steady state and to begin a periodic oscillation; the development of more complex, aperiodic oscillations; the re-establishment of periodic oscillation but with a different wavelength and frequency; a final return to the steady state as the wave packet passes beyond the point of observation. The directional flow imposes a 'preferred' direction and, hence, breaks the symmetry of the reactor as a whole.

The CGL equation has previously been used successfully to determine aspects of the spatiotemporal evolution of chemical systems close to the interaction of bifurcation points. In particular, the Brussels group has used this approach to give a full account of the Turing–Hopf interactions^{23–25} and has recently considered the influence of a uniform flow on this behaviour.²⁶ A survey of the CGL equation, as applied to chemical systems, has been given by Ipsen.²⁷ Our conditions are at the other extreme from the Turing condition: here $D_B \gg D_A$ pertains, and so we have the interaction of convective and oscillatory instabilities. Rovinsky *et al.*¹⁷ used the

CGL equations to investigate the dependence of the most stable wavenumber k on the flow velocity, showing wavelength locking with a particular wavenumber k^* , stable over a range of flow rate, and the system then jumping to a new wave number $2k^*$ as the flow is increased beyond some bifurcation value. Such behaviour is not a feature of the present study, in which we observed a continuous variation of the selected wavenumber on ψ . This difference arises from the different boundary conditions imposed in the two studies. Rovinsky *et al.* employed periodic boundary conditions and, thus, imposed a specific length scale on the system. Here, we have effectively an infinite domain probably corresponding more closely to real reactor systems.

Rovinsky *et al.* also mentioned the observation of complex responses in their computations, which they ascribe as arising through the so-called Benjamin–Feir (BF) instability²⁸ which is associated, in fluid mechanics, with the break-up of wave trains in deep water. The condition for this particular instability can be written explicitly in terms of the coefficients in the CGL equation and they arranged to study parameter values satisfying this condition. Our own computations described above also lie within this parameter domain, but we have performed further computations based on the CGL equation appropriate to the more general form of the mass balance equations

$$\frac{\partial a}{\partial t} = \delta \left(\frac{\partial^2 a}{\partial x^2} - \phi \frac{\partial a}{\partial x} \right) \mu - ab^2 \quad (17)$$

$$\frac{\partial b}{\partial t} = \frac{\partial^2 b}{\partial x^2} - \phi \frac{\partial b}{\partial x} + ab^2 - b \quad (18)$$

where δ gives the relative mobility of A with respect to B. By increasing δ sufficiently far from zero, we leave the BF domain and we observe that the basic phenomena reported here remain over a wide range of parameter values outside the BF domain. Interestingly, this subsequent work has shown that the basic response of two regions of simple evolution separated by a region of chaos depends specifically on neither the differential aspect ($\delta \neq 1$) nor on the flow ($\psi \neq 0$). Fig. 7 shows the amplitude $|A|$ and reconstructed autocatalyst concentration for a system with $\delta = 1$ and $\phi = 0$. In this case, the absence of flow means that the wave packet is not itself propagating and there is symmetry about $s = 0$, so that the 'front' and 'rear' (now right- and left-propagating) regions of simple behavior have the same wavelength. Despite having the same wavelength in these two regions, the system still develops a region of spatiotemporal chaos centred on the origin, driven solely by the interaction of the Hopf bifurcation and (equal) diffusion. This result suggests that the instability mechanism is not of the BF type but may be related to the wave-induced chaos reported previously^{29,30} in a related system. Here, however, rather than having a simple front propagating ahead of the chaotic region, there is a growing wave train. We may, however, also note that the timescale on which the chaotic behaviour develops does appear to depend on the flow component, decreasing as ψ increases.

Some insight into why the region of chaotic behaviour develops between the regions of regular wave trains may be obtained by noting that, in its initial development, the amplitude remains almost constant. If we express the complex amplitude A in the amplitude-phase form $A = R \exp i\theta$ and assume that R is a constant, we get, from eqn. (11)

$$3 \frac{\partial \theta}{\partial \tau} = - \frac{\partial^2 \theta}{\partial s^2} + 4 \left(\frac{\partial \theta}{\partial s} \right)^2 + \psi \frac{\partial \theta}{\partial s} - 8 \quad (19)$$

describing the evolution of the phase $\theta(s, \tau)$ during this initial period. This is an equation of the Kuramoto–Sivashinsky^{31,32} type. The 'negative phase diffusion' in eqn. (19) means that any perturbation to the phase will be highly unstable, suggesting the development of 'phase turbulence'. This instability is

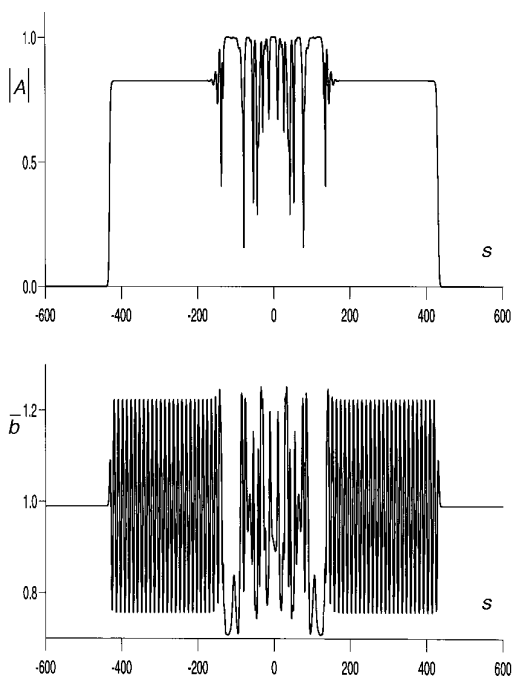


Fig. 7 Amplitude $|A|$ and reconstructed autocatalyst concentration profiles for simple diffusive CGL equation ($\delta = 1$ and $\psi = 0$) showing symmetric wave packet evolving from $s = 0$ with two regions of constant amplitude and (the same) wavelength connected by a growing region of spatiotemporal chaos

the most likely source for the subsequent development, on a longer timescale, of the 'amplitude turbulence', where R is no longer constant and the full non-linearity of the system comes into play.

As a formal, final point, it should be mentioned that the spatiotemporal chaos does not arise through an 'interaction' of the bifurcation modes in the strict mathematical sense. This is not a codimension-2 phenomenon and is a new response for the basic CGL equations, even without the differential flow.

References

- 1 A. M. Turing, *Phil. Trans. R. Soc. London B*, 1952, **327**, 37.
- 2 N. Rashevski, *Mathematical Biophysics*, University of Chicago Press, Chicago, 1938.

- 3 P. Glansdorff and I. Prigogine, *Thermodynamic Theory of Structure, Stability and Fluctuations*, Wiley, New York, 1971.
- 4 J. D. Murray, *Mathematical Biology*, Springer, Berlin 1989.
- 5 P. Borckmans, G. Dewel, A. De Wit and D. Walgraef, in *Chemical Waves and Patterns*, ed. R. Kapral and K. Showalter, Kluwer, Dordrecht, 1995, p. 221.
- 6 P. K. Maini, K. J. Painter and H.N.P. Chau, *J. Chem. Soc., Faraday Trans.*, 1997, **93**, 3601.
- 7 B. R. Johnson and S. K. Scott, *Chem. Soc. Rev.*, 1996, **93**, 265.
- 8 V. Castets, E. Dulos, J. Boissonade and P. De Kepper, *Phys. Rev. Lett.*, 1990, **64**, 2953.
- 9 Q. Ouyang and H. L. Swinney, *Chaos*, 1991, **1**, 411.
- 10 I. Lengyel and I. R. Epstein, *Science*, 1991, **251**, 650.
- 11 A. B. Rovinsky and M. Menzinger, *Phys. Rev. Lett.*, 1992, **69**, 1193.
- 12 A. B. Rovinsky and M. Menzinger, *Phys. Rev. Lett.*, 1993, **70**, 778.
- 13 P. Gray and S. K. Scott, *Ber. Bunsen-Ges. Phys. Chem.*, 1986, **90**, 985.
- 14 J. H. Merkin, D. J. Needham and S. K. Scott, *Proc. R. Soc. London A*, 1986, **406**, 299.
- 15 R. A. Satnoianu, J. H. Merkin and S. K. Scott, *Physica D*, in press.
- 16 R. A. Satnoianu, J. H. Merkin and S. K. Scott, *Phys. Rev. E*, in press.
- 17 A. Rovinsky, A. Malevanets and M. Menzinger, *Physica D*, 1996, **95**, 306.
- 18 M. C. Cross and P. C. Hohenberg, *Rev. Mod. Phys.*, 1993, **65**, 851.
- 19 R. J. Deissler, *J. Stat. Phys.*, 1985, **40**, 373.
- 20 M. V. Bazhenov, M. I. Rabinovich and A. L. Fabrikant, *Phys. Lett. A*, 1992, **163**, 87.
- 21 K. Nozaki and N. Bekki, *J. Phys. Soc. Jpn.*, 1984, **53**, 1581.
- 22 H. Sakaguchi, *Prog. Theor. Phys.*, 1991, **85**, 417.
- 23 A. De Wit, G. Dewel and P. Borckmans, *Phys. Rev. E*, 1993, **48**, 4191.
- 24 A. De Wit, D. Lima, G. Dewel and P. Borckmans, *Phys. Rev. E*, 1996, **54**, 261.
- 25 M. Meixner, A. De Wit, S. Bose and E. Scholl, *Phys. Rev. E*, 1997, **55**, 6690.
- 26 S. P. Kuznetsov, E. Mosekilde, G. Dewel and P. Borckmans, *J. Chem. Phys.*, 1997, **106**, 7609.
- 27 M. Ipsen, Ph.D. thesis. University of Copenhagen. 1996.
- 28 T. B. Benjamin and J. E. Feir, *J. Fluid Mech.*, 1967, **27**, 417.
- 29 J. H. Merkin, V. Petrov, S. K. Scott and K. Showalter, *Phys. Rev. Lett.*, 1996, **76**, 546.
- 30 J. H. Merkin, V. Petrov, S. K. Scott and K. Showalter, *J. Chem. Soc., Faraday Trans.*, 1996, **92**, 2911.
- 31 Y. Kuramoto, *Chemical Oscillations, Waves and Turbulence*, Springer-Verlag, Berlin, 1984.
- 32 G. I. Sivashinsky, *Annu. Rev. Fluid Mech.*, 1983, **15**, 179.

Paper 7/09156G; Received 22nd December, 1997